

Fe-based nanocrystalline soft magnetic alloys for high-temperature applications

Keith E. Knipling,^{a)} Maria Daniil, and Matthew A. Willard

U.S. Naval Research Laboratory, Multifunctional Materials Branch, 4555 Overlook Ave. SW, Washington, District of Columbia 20375, USA

(Received 20 July 2009; accepted 30 October 2009; published online 4 December 2009)

We report on improved high-temperature soft magnetic properties in $\text{Fe}_{88-2x}\text{Co}_x\text{Ni}_x\text{Zr}_7\text{B}_4\text{Cu}_1$ nanocrystalline alloys. Substituting 5.5 at. % Co and Ni for Fe enhances the magnetization by 5% at ambient temperature and by 30% at 650 °C. The Curie temperature of the residual amorphous phase is also raised significantly (from 67 °C for $x=0$ to 298 °C for $x=5.5$), resulting in low coercivities ($<30 \text{ A m}^{-1}$) for $\text{Fe}_{77}\text{Co}_{5.5}\text{Ni}_{5.5}\text{Zr}_7\text{B}_4\text{Cu}_1$ over the temperature range 50–500 °C. The higher magnetization and Curie temperature as compared with other Fe-based alloys, and smaller Co content as compared with (Fe,Co)-based alloys, make this alloy attractive as an affordable high-temperature soft magnetic material. © 2009 American Institute of Physics. [doi:10.1063/1.3268471]

Nanocrystalline soft magnetic alloys are promising materials for use in high frequency inductor, power transformer, flux gate magnetometer, and rotors for electric motor applications.¹ They are typically produced from amorphous precursors that are partially devitrified, resulting in nanoscale ferromagnetic grains embedded in a residual ferromagnetic amorphous matrix. When the grains are smaller than the exchange correlation length and their orientation is random, the magnetocrystalline anisotropy is averaged out by exchange interactions and the alloys possess a unique combination of large magnetization, high permeability, and low core losses.² The exchange-coupling is reduced, however, as the operation temperature approaches the Curie temperature of the intergranular amorphous phase, thus limiting applicability of existing Fe-based alloys (e.g., Finemet-type $\text{Fe}_{73.5}\text{Si}_{13.5}\text{Nb}_3\text{B}_9\text{Cu}_1$ or Nanoperm-type $\text{Fe}_{88}\text{Zr}_7\text{B}_4\text{Cu}_1$) to moderate temperatures ($T \lesssim 300 \text{ °C}$).

Magnetic alloys have been developed for elevated-temperature use. These include HiTperm alloys ($\text{Fe}_{44}\text{Co}_{44}\text{Zr}_7\text{B}_4\text{Cu}_1$) possessing a large Curie temperature of both constituent phases (i.e., the α -FeCo grains and the amorphous matrix), resulting in low coercivity and large magnetization at elevated temperatures.^{3,4} The Co additions, however, increase the coercivity and core losses due to increased magnetostriction.⁵ Further substitutions of Co for Fe in HiTperm decrease the coercivity while maintaining a high Curie temperature, but the magnetization is significantly reduced.^{6,7} Furthermore, Co is relatively expensive making these nanocrystalline alloys less attractive economically than Fe-based ones. In this letter, we report on an Fe-rich alloy with greatly improved high-temperature performance with small Co additions.

High purity elemental constituents in the appropriate weight ratios were arc-melted in a gettered argon atmosphere, producing homogeneous button ingots approximately 25 g in mass. Amorphous ribbons, typically 2–3-mm-wide and 20- μm -thick, were produced by inductively melting the button ingots in a partial helium atmosphere and ejecting the

melt through a 0.7–0.8 mm orifice onto the perimeter of a copper wheel rotating at a surface speed of 50 m s^{-1} . The ribbons were isothermally annealed at 550 °C for 3600 s in an argon atmosphere to partially devitrify the alloys into their optimum microstructure for best magnetic performance.

The crystal structure of the as-spun and annealed ribbons was examined by x-ray diffraction (XRD) using a Philips APD 3520 diffractometer with $\text{Cu K}\alpha$ radiation ($2\theta=20\text{--}120^\circ$). The mean size of the Fe-based nanocrystalline phase was estimated from the half-peak breadth of the $\{110\}$, $\{200\}$, $\{211\}$, $\{220\}$, and $\{310\}$ XRD peaks via the Scherrer equation, and the lattice parameter was determined using the $\cos^2 \theta / \sin \theta$ method.⁸

Quasistatic magnetic hysteresis loops were measured at ambient and elevated temperatures (50–650 °C) using an ADE model 4HF vibrating sample magnetometer (VSM) with a maximum applied field of $7.96 \times 10^5 \text{ A m}^{-1}$ (10 kOe). Thermomagnetic measurements of the as-spun alloys were performed at a fixed applied field of $3.18 \times 10^5 \text{ A m}^{-1}$ (4 kOe). The ribbon samples for magnetometry were approximately 7 mm in length and aligned with the applied field direction during measurement.

The as-spun ribbons were completely amorphous, as confirmed by XRD (Fig. 1). After annealing at 550 °C for 3600 s, broad reflections from the Fe-rich body-centered cubic (bcc) crystallites are observed. The lattice parameters of the nanocrystalline grains were determined to be 0.2870 and 0.2874 nm for $\text{Fe}_{88}\text{Zr}_7\text{B}_4\text{Cu}_1$ and $\text{Fe}_{77}\text{Co}_{5.5}\text{Ni}_{5.5}\text{Zr}_7\text{B}_4\text{Cu}_1$, respectively. The estimated grain size in both alloys is 11–12 nm.

Thermomagnetic curves of magnetization M , as a function of temperature, are shown in Fig. 2 for the as-spun alloys. Both curves exhibit similar behavior, with an initial decrease in M with increasing temperature, corresponding to the ferromagnetic-paramagnetic phase transformation of the amorphous as-spun ribbons. The Curie temperature of the amorphous phase T_C^{am} is much higher for $\text{Fe}_{77}\text{Co}_{5.5}\text{Ni}_{5.5}\text{Zr}_7\text{B}_4\text{Cu}_1$ (289 °C) than it is for $\text{Fe}_{88}\text{Zr}_7\text{B}_4\text{Cu}_1$ (67 °C). This is a critical parameter for high-temperature applications, since the magnetic properties deteriorate above T_C^{am} due to the reduced exchange-coupling between adjacent

^{a)}Electronic mail: knipling@anvil.nrl.navy.mil.

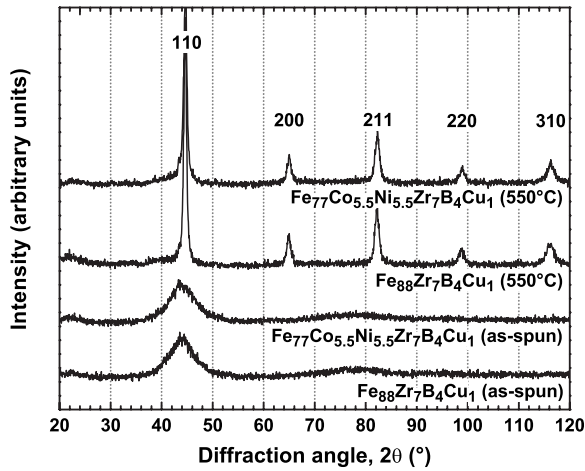


FIG. 1. XRD data for the Fe₈₈Zr₇B₄Cu₁ and Fe₇₇Co_{5.5}Ni_{5.5}Zr₇B₄Cu₁ alloys in the as-spun and annealed conditions.

grains through the increasingly paramagnetic amorphous matrix phase. When this happens, the coercivity of the nanostructured material increases significantly. This increase, however, is reversible so long as no structural changes accompany the temperature rise.

In Fe-based alloys, metalloids (e.g., P, B) or early transition metals (e.g., Zr, Hf, Nb) are the most commonly used glass forming elements, and T_C^{am} generally increases as the Fe content decreases⁹ due to local correlation effects in the amorphous alloy.¹⁰ Alloys with metalloid additions have strong hybridization of the metalloid p -orbitals with the Fe d -orbitals, which shifts the maximum in the density of states to lower energies, thereby decreasing the ground state magnetization and T_C^{am} . With early transition metal additions, the changes in the density of states is linked to a reduction in coordination number with increasing transition metal content due to its larger atomic size. The T_C^{am} values we observe for Fe₈₈Zr₇B₄Cu₁ (67 °C) and Fe₇₇Co_{5.5}Ni_{5.5}Zr₇B₄Cu₁ (289 °C) are consistent with the above considerations, having smaller values than Fe-poor alloys (e.g., Fe₈₀B₁₀P₁₀, $T_C^{\text{am}}=347$ °C¹¹) and larger values than Fe-rich alloys (e.g., Fe₉₀Zr₁₀, $T_C^{\text{am}}=-48$ °C¹²) alloys. Previous studies in other ferromagnetic amorphous alloys (both metalloid and early transition metal systems) have

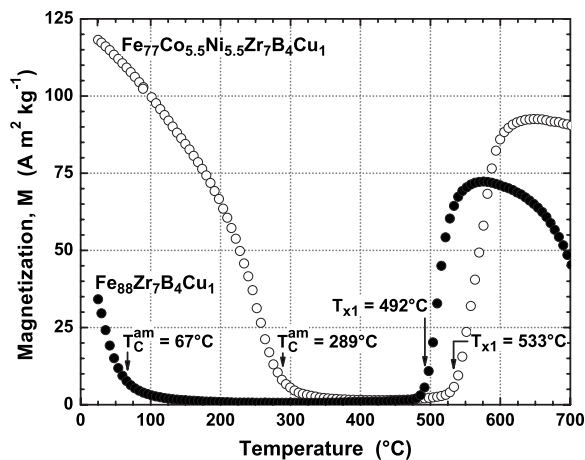


FIG. 2. Magnetization as a function of temperature for the as-spun Fe₈₈Zr₇B₄Cu₁ and Fe₇₇Co_{5.5}Ni_{5.5}Zr₇B₄Cu₁ alloys ($H_{\text{max}}=3.18 \times 10^5$ A m⁻¹).

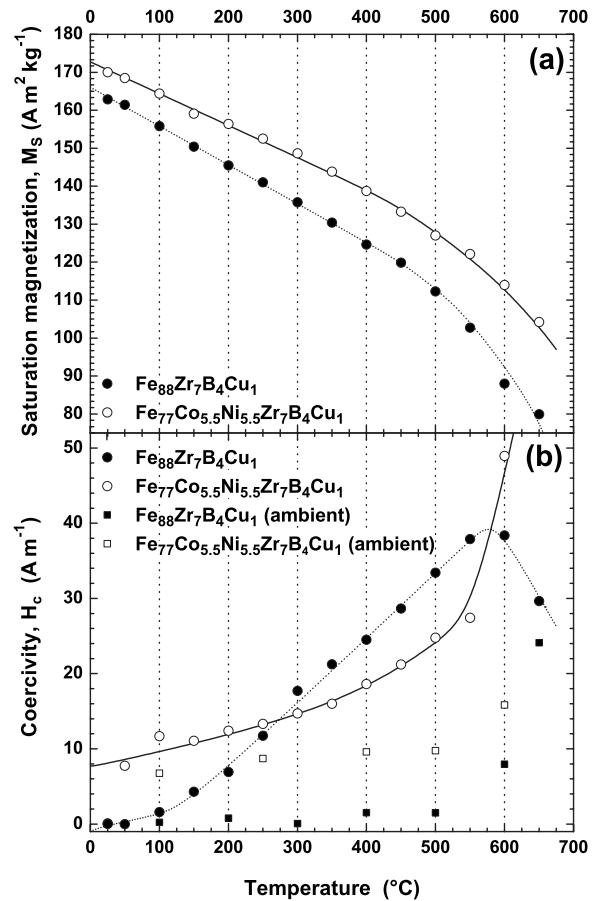


FIG. 3. Temperature dependence of M_s (a) and H_c (b) for the Fe₈₈Zr₇B₄Cu₁ and Fe₇₇Co_{5.5}Ni_{5.5}Zr₇B₄Cu₁ alloys annealed at 550 °C for 3600 s ($H_{\text{max}}=7.96 \times 10^5$ A m⁻¹).

shown that small substitutions of Ni and (especially) Co increase T_C^{am} ,^{11,12} which is attributed to a minimum in the spin wave density of states for low energy spin waves.¹³ This explains the improved T_C^{am} for Fe₇₇Co_{5.5}Ni_{5.5}Zr₇B₄Cu₁ as compared with Fe₈₈Zr₇B₄Cu₁. It should also be noted that T_C^{am} in nanocrystalline alloys is generally greater than that of the amorphous precursor, due to enrichment in metalloid and early transition metal atoms in the intergranular amorphous phase, as well as exchange penetration from the nanocrystallites through the significant nanocrystalline/amorphous interfacial area.^{9,14}

Beyond T_C^{am} the magnetization falls to zero (Fig. 2) confirming the lack of crystalline phase in the as-spun ribbons. At higher temperatures the curves exhibit an abrupt increase in M , corresponding to primary crystallization of the ferromagnetic bcc grains from the amorphous matrix ($T_{x1} \sim 500$ °C for both alloys). Beyond 600 °C, M decreases again as the temperature approaches that of the Curie temperature of the crystalline phase (above our maximum measurement temperature of 700 °C).

To assess the viability of these alloys for high-temperature use, hysteresis loops were measured at ambient temperature (25 °C) and every 50 °C from 50–650 °C. The observed saturation magnetization M_s and coercivity H_c are shown in Figs. 3(a) and 3(b), respectively. At all temperatures, substituting Co and Ni for Fe increases the M_s , with the relative benefit increasing with increasing temperature. At ambient temperature, the M_s of Fe₇₇Co_{5.5}Ni_{5.5}Zr₇B₄Cu₁ is

5% greater than that of $\text{Fe}_{88}\text{Zr}_7\text{B}_4\text{Cu}_1$, which increases to 10% at 300 °C and 30% at 600 °C.

Figure 3(b) shows the effect of temperature on H_c . The soft magnetic properties deteriorate with increasing temperature due to reduced exchange-coupling of the ferromagnetic grains through the intergranular amorphous phase, which becomes paramagnetic near 67 °C for $\text{Fe}_{88}\text{Zr}_7\text{B}_4\text{Cu}_1$ or 289 °C for $\text{Fe}_{77}\text{Co}_{5.5}\text{Ni}_{5.5}\text{Zr}_7\text{B}_4\text{Cu}_1$ (Fig. 2). Because of the higher T_C^{am} value, H_c increases at a much slower rate for the alloy containing Co and Ni. Thus, while $\text{Fe}_{88}\text{Zr}_7\text{B}_4\text{Cu}_1$ exhibits significantly smaller losses than $\text{Fe}_{77}\text{Co}_{5.5}\text{Ni}_{5.5}\text{Zr}_7\text{B}_4\text{Cu}_1$ at lower temperatures ($T \leq 250$ °C), better soft magnetic properties are obtained for the latter alloy at 350–500 °C. The magnetocrystalline anisotropy is expected to be small for both alloys, and the larger H_c observed for $\text{Fe}_{88}\text{Zr}_7\text{B}_4\text{Cu}_1$ at 350–500 °C is likely due to an increase in magnetostriction, which has been measured at room temperature to be ~ 1 and ~ 2.5 ppm for $\text{Fe}_{88}\text{Zr}_7\text{B}_4\text{Cu}_1$ and $\text{Fe}_{77}\text{Co}_{5.5}\text{Ni}_{5.5}\text{Zr}_7\text{B}_4\text{Cu}_1$, respectively.

The H_c values for $\text{Fe}_{77}\text{Co}_{5.5}\text{Ni}_{5.5}\text{Zr}_7\text{B}_4\text{Cu}_1$ [Fig. 3(b)] remain well below 20 A m⁻¹ to 300 °C and are below 30 A m⁻¹ out to 550 °C. Škorvánek *et al.*¹⁵ and Sun *et al.*¹⁶ recently performed similar experiments on HiTperm-type alloys and observed much larger values of H_c over this temperature range (~ 25 and 48 A m⁻¹, respectively). While M_s was not reported in these studies, values as large as 180 A m² kg⁻¹ have been reported for HiTperm alloys,¹⁷ which is comparable to that observed for our alloys [Fig. 3(a)].

Figure 3 also shows ambient temperature H_c measurements performed after the sample had been cooled from the elevated test temperature. For both alloys, the ambient-temperature H_c measured after exposure to $T \leq 500$ °C is comparable to that measured initially at 25 °C, indicating that the increase in H_c with temperature is due to thermal fluctuations and is not permanent. Above 500 °C there is an irreversible change in H_c , which may indicate a partial crystallization of the residual amorphous phase and/or coarsening of the nanocrystalline grains. Differential thermal analysis results (not shown) indicate that the secondary crystallization temperature exceeds 730 °C for these alloys, suggesting that the latter explanation is more likely. This irreversible struc-

tural change limits the operation temperature of the alloys to ~ 500 °C.

Additions of 5.5 at. % Co and Ni to Nanoperm-type ($\text{Fe}_{88}\text{Zr}_7\text{B}_4\text{Cu}_1$) soft magnetic alloys dramatically increase the Curie temperature of the intergranular amorphous phase (from 67 °C for $\text{Fe}_{88}\text{Zr}_7\text{B}_4\text{Cu}_1$ to 289 °C for $\text{Fe}_{77}\text{Co}_{5.5}\text{Ni}_{5.5}\text{Zr}_7\text{B}_4\text{Cu}_1$), resulting in greater exchange-coupling and a commensurate reduction in coercivity over the temperature range 300–500 °C. The small additions of Co and Ni also enhance the magnetization at all temperatures investigated (25–650 °C). The maximum operational temperature of the alloys is approximately 500 °C, beyond which the alloys undergo irreversible structural changes (most likely grain coarsening). The relatively small Co and Ni contents makes this high-temperature, high-performance soft magnetic alloy particularly attractive from an economic standpoint, as compared with existing Co-rich alloys.

This research is supported by the Office of Naval Research under contract N00014-09-WX-2-0658

- ¹M. E. McHenry, M. A. Willard, and D. E. Laughlin, *Prog. Mater. Sci.* **44**, 291 (1999).
- ²G. Herzer, *J. Magn. Magn. Mater.* **112**, 258 (1992).
- ³M. A. Willard, D. E. Laughlin, M. E. McHenry, D. Thoma, K. Sickafus, J. Cross, and V. G. Harris, *J. Appl. Phys.* **84**, 6773 (1998).
- ⁴M. E. McHenry and D. E. Laughlin, *Acta Mater.* **48**, 223 (2000).
- ⁵F. Johnson, C. Um, M. McHenry, and H. Garmestani, *J. Magn. Magn. Mater.* **297**, 93 (2006).
- ⁶M. A. Willard, J. Claassen, R. Stroud, T. Francavilla, and V. G. Harris, *IEEE Trans. Magn.* **38**, 3045 (2002).
- ⁷M. Daniil and M. A. Willard, *J. Appl. Phys.* **103**, 07E727 (2008).
- ⁸B. Cullity, *Elements of X-Ray Diffraction*, 2nd ed. (Addison-Wesley, Reading, 1978).
- ⁹A. Hernando, I. Navarro, and P. Gorriá, *Phys. Rev. B* **51**, 3281 (1995).
- ¹⁰Y. Kakehashi, *Mater. Sci. Eng., A* **179**, 62 (1994).
- ¹¹T. Mizoguchi, *AIP Conf. Proc.* **34**, 286 (1976).
- ¹²S. Bao-gen, X. Rufeng, Z. Jian-Gao, and Z. Wen-Shan, *Phys. Rev. B* **43**, 11005 (1991).
- ¹³R. Hasegawa and J. Dermon, *Phys. Lett. A* **42**, 407 (1973).
- ¹⁴A. Yavari and D. Negri, *Nanostruct. Mater.* **8**, 969 (1997).
- ¹⁵I. Škorvánek, P. Svec, J. Marcin, J. Kovac, T. Krenicky, and M. Deanko, *Phys. Status Solidi A* **196**, 217 (2003).
- ¹⁶Y. Sun, L. Zhong, and X. Bi, *Scr. Mater.* **60**, 814 (2009).
- ¹⁷H. Iwanabe, B. Lu, M. McHenry, and D. Laughlin, *J. Appl. Phys.* **85**, 4424 (1999).